Communication in Physical Sciences, 2024, 11(4): 711-720

Pore Parameters Analysis of *Echinochloa pyramidalis* leaf Dopped Silver Nanoparticles

Nyeneime William Akpanudo* and Ojeyemi Matthew Olabemiwo
Received: 02 April 2024/Accepted: 18 August 2024/ Published: 25 August 2024

Abstract: *Nanoparticles are significant products that have attracted a high level of market demand because of their outstanding surface properties. Silver nanoparticles are preferred in numerous industrial applications including water purification because of their thermal stability, particle size, surface area and other pore properties. In this study, silver nanoparticles (AgNPs) were synthesised using leaf extract of Echinochloa pyramidalis and later doped with the powder leaf sample. The products were analysed for their fundamental properties (i.e surface and pore properties) using nitrogen adsorption methods based on the BET models. The results, derived from Density Functional Theory (DFT) and differential pore volume (dV(d)) data, reveal that AgNPs exhibit a mesoporous structure with pore diameters ranging from 1.7656 to 2.7691 nm. The cumulative pore volume increases with pore width, reaching 5.52 × 10⁻² cm³/g, while the cumulative surface area grows to 47.1 m²/g, indicating a broad distribution of pore sizes. The differential analysis identifies key pore diameters at 2.3129, 2.4194, 2.5307, and 2.6472 nm as significant contributors to the material's pore volume and surface area. The average pore diameter is calculated to be approximately 4.69 nm. Langmuir and BET models for nitrogen adsorption provide surface area estimates of 522.586 m²/g and 167.780 m²/g, respectively, highlighting the high surface area to volume ratio of the nanoparticles. The findings confirm that the mesoporous nature of AgNPs, with a diverse range of pore sizes contribute to their significant surface area and adsorption capacity.*

Keywords*: Silver nanoparticles, pore analysis, N_2 adsorption, surface application*

Nyeneime William Akpanudo
Department of Chemistry, Akwa Ibom State University, Ikot Akpaden, Ikot Abasi, Akwa Ibom State, Nigeria.
Email: nyewills15@gmail.com
Orcid id: 0000-0001-8095-6667

Ojeyemi Matthew Olabemiwo
Department of Pure and Applied Chemistry, Ladoke Akintola University of Technology, Ogbomoso, Nigeria
Email: omolabemiwo@lautech.edu.ng

1.0 Introduction

Nanotechnology has gone above most fields in materials science, concerning applications and provision of innovations to various industries due to their unique properties (Ogoko *et al*. 2023). Most materials that could complement or act as suitable replacements have been reported to suffer from some setbacks that could hinder their applications, such as ease of oxidation or reaction (describing chemical instability), thermal instability, band gap/electron-hole recombination, mechanical instability, irreversibility, solubility, low surface areas, poor electrical conductivity, unpredicted (Dauthal and Mukhopadhyay 2016). Several metal-based nanoparticles are found in the combined states such as CaO, MgO, TiO_2, CuO, MnO_2, ZnO, AgO, SnO_2, CuO, Al_2O_3, CeO_2, ZrO_2 etc (Nazir *et al*. 2024). However, silver nanoparticles (AgNPs) have garnered significant attention due to their exceptional physicochemical properties, including high surface area, chemical stability, thermal stability, and versatile pore structures.

These properties make AgNPs highly suitable for applications in water purification, catalysis, medical devices, and electronics (Khan *et al.* 2020; Singh *et al*. 2021).

The synthesis of AgNPs using biological methods, often termed "green synthesis" has gained prominence over conventional chemical and physical methods due to its eco-friendliness, cost-effectiveness, and simplicity. Plant extracts, in particular, have been extensively explored for this purpose as they provide a rich source of reducing agents and stabilizers. *Echinochloa pyramidalis*, a common wetland grass, has shown potential in synthesizing nanoparticles due to its abundant phytochemicals that facilitate the reduction and stabilization of metal ions (Akpanudo and Olabemiwo 2024a, b; Ahmed *et al*. 2022).

The synthesis and characterization of AgNPs have been the focus of numerous studies, with a significant emphasis on understanding their surface and pore properties. Recent research has highlighted the importance of these properties in determining the efficacy of AgNPs in various applications. Lee *et al*. (2019) observed that AgNPs are mesoporous and were able to enhance the catalytic degradation of environmental contaminants. In our previous work, we observed an average % removal of PAHs by AgNPs from bitumen seepage water to be above 90% (Akpanudo and Olabemiwo 2024b). Similarly, Zhang *et al.* (2020) reported that the adsorption capacity of AgNPs in water treatment applications is directly influenced by their surface area and pore volume. AgNPs have also been found to be effective in other sectors including semiconductor and electrical industries (Eddy *et al*., 2024a). In all forms of applications of nanoparticles including silver nanoparticles, the first set of parameters that need to be considered is surface properties such as particle size, surface area, pore volume, surface area to pore volume ratio and others (Ngosi *et al*., 2024). These parameters are fundamental because they can have significant impacts on other parameters (such as porosity, density, crystallite size, etc) and hence their potential applications.

One of the founded methodologies for the determination of pore parameters is the nitrogen adsorption process based on the Brunauer-Emmett-Teller (BET model (Eddy *et al*., 2024b). The fundamental of the model is rooted in the investigation of adsorption parameters such as the mass of adsorbed, pressure of the gas and surface coverage (ref). Once these fundamental parameters are determined, the next step is to fit adsorption isotherms. One of the major challenges facing the employment of this model in the determination of pore parameters is the ability to choose the best-fitted isotherm. Consequently, some literature are confronted with good experimental results but little accuracy due to the inability to extract data from the most suitable isotherm. In this work, we present the various isotherms resulting from the nitrogen adsorption studies on *Echinochloa pyramidalis* leaf-dopped silver nanoparticles (AgNC-L). The isotherms are analysed and the choice of best-fitted isotherms are presented.

Several studies have employed the Brunauer-Emmett-Teller (BET) model and Density Functional Theory (DFT) to analyze the surface and pore properties of AgNPs. For example, Mishra *et al*. (2021) utilized BET and DFT models to determine the pore size distribution and surface area of biosynthesized AgNPs, revealing a broad range of pore sizes that contribute to their high surface area. Moreover, differential pore volume (dV(d)) and differential surface area (dS(d)) analyses have been pivotal in identifying the dominant pore sizes that significantly impact the overall properties of the nanoparticles (Gupta *et al*., 2022).

Despite the extensive research on the synthesis and characterization of AgNPs, there remains a knowledge or (research) gap in the comprehensive analysis of pore parameters, especially for nanoparticles synthesized using

less commonly studied plant species like *Echinochloa pyramidalis*. While previous studies have focused on popular plant extracts, the potential of *Echinochloa pyramidalis* in synthesizing AgNPs with unique pore properties has not been fully explored.

This study aims to synthesize AgNPs using the leaf extract of *Echinochloa pyramidalis* and subsequently dope them with the same powder leaf extract. The analysis of the fundamental surface and pore properties of the synthesized AgNPs using nitrogen adsorption methods shall be based on the BET models. The findings of this study can provide insights into the potential of *Echinochloa pyramidalis* leaf extract in synthesizing AgNPs with desirable pore properties. Consequently, the results can be crucial for optimizing the use of AgNPs in various industrial applications, particularly in water purification and environmental remediation.

2.0 Materials and Methods

Echinochloa pyramidalis plant was collected from the teaching and research farm of Akwa Ibom State University. The uprooted plant was thoroughly washed repeatedly with tap water followed by double distilled water to remove dust particles and set aside to dry at room temperature (30 ± 2°C) for 15 days (Murthy *et al*. 2020) to remove moisture contents from the samples. The leaf sample was milled or ground into powder form and preserved. Aqueous extract of the leaf was prepared by soaking the powder sample in 250 ml of distilled water and allowed to stand for 30 mins. The filtrate was obtained and stored in the refrigerator for further use. The reduction of 30 mM (Alshammari *et al*. 2023) of $AgNO_3$ to silver nanoparticles was initiated by the addition of the leaf extract in the ratio of 50 ml of the extract to 50 ml of the nitrate solution (Jalab *et al.* 2021). Stirring was initiated while the reaction system was maintained at (25 ± 2°C) 298 K for 2 hours. The reduction process from Ag^+ to Ag^0 which indicates the formation of silver nanoparticles AgNP (Jadoun *et al.* 2021; Rather *et al*. 2022) was confirmed by the visual observation of the colour change (ie, the appearance of light brown and finally dark brown colour) and measurement of the absorbance spectrum of the reaction mixture using UV-Vis spectrometer V1.63.0. The reaction was maintained at pH 8 because the hydroxyl ions in the alkaline media could accelerate the transfer of electrons from phytochemical compounds in the extract to metal ions (Zayed *et al.* 2015). The nanoparticles obtained were incubated at 311 K before they were thoroughly washed with distilled water and dried for 12 h in a vacuum at 343 K. Nanocomposites of silver (Ag-NCs) were also prepared by mixing 10ml of 0.042 mg/L solution of freshly prepared silver nanoparticles with 15.0g of the dried leaf sample, followed by oven drying at 353 K.

The analysis of the pore properties was conducted with a BET analyser to investigate the nitrogen adsorption properties of the nanoparticles and the composites considering different adsorption models including Dubinin–Ashtakov (D–A), Dubinin–Radushkevich (D–R), Barrett–Joyner–Halenda (B–JH), Langmuir (Langm), density functional theory (DFT) and Horvath–Kawazoe (HK) methods (Dudnikova *et al.* 2021). Evaluated pore properties included pore volume, surface area and pore size. The adsorption energy was also evaluated from the D–R isotherm.

3.0 Results and Discussion

Fig. 1 shows the plots of cumulative pore volume versus pore diameter and cumulative surface area versus pore diameter based on the DFT analysis of nitrogen adsorption by AgNC-L. In Fig. 2 plots of differential pore volume (dV(d)) versus pore diameter and differential surface area (dS(d)) versus pore diameter (based on the DFT model) are also provided. The data obtained for pore diameter ranges from 1.7656 nm to 2.7691 nm. The cumulative pore volume (cm^3/g) is observed to increase as the pore width increases, indicating the

accumulation of pore volume (Fig. 1a). Also, the cumulative surface area (m^2/g) increases with an increase in the pore diameter. The differential pore volume(dV(d) ($cm^3/g/nm$) represents the change in pore volume per unit change in pore width while the differential surface area dS(d) ($m^2/g/nm$):, represents the change in surface area per unit change in pore width.

The observed range for pore diameter indicates that the AgNC-L is a mesoporous material since the pore size ranges from 2 to 50 nm. The increase in both cumulative pore volume and cumulative surface area with pore width suggests a broad distribution of pore sizes within the measured range. The cumulative pore volume starts at 1.76E-03 cm^3/g and reaches 5.52E-02 cm^3/g at the maximum pore width. Also, the cumulative surface area increases from 2.21 m^2/g to 47.1 m^2/g. These trends indicate that larger pore sizes contribute significantly to the total pore volume and surface area.

The differential pore volume peaks at certain pore widths signalled where the majority of the pore volume is distributed. Observable peaks are at pore diameters of 2.3129, 2.4194, 2.5307, and 2.6472 nm, which suggests that the listed pore diameters are dominant in the sample..

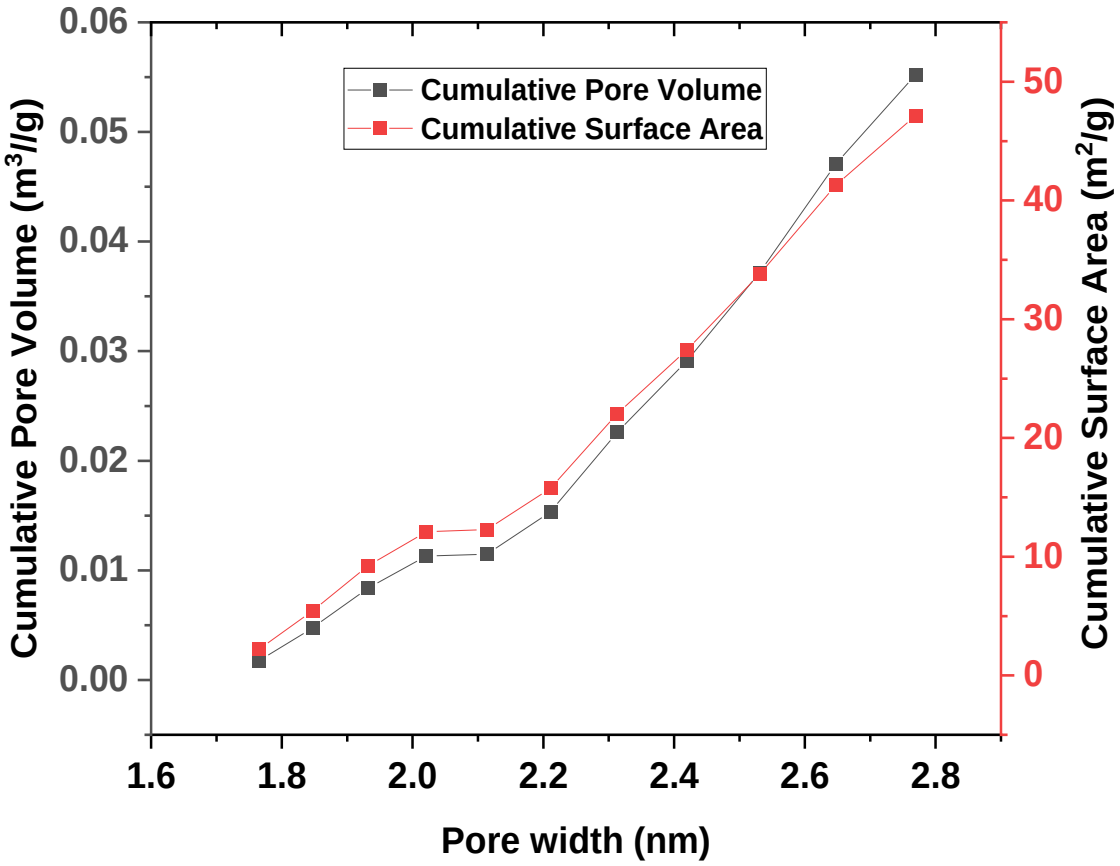

Fig. 1: DFT plots for the variation of cumulative pore volume and cumulative pore surface with pore diameter

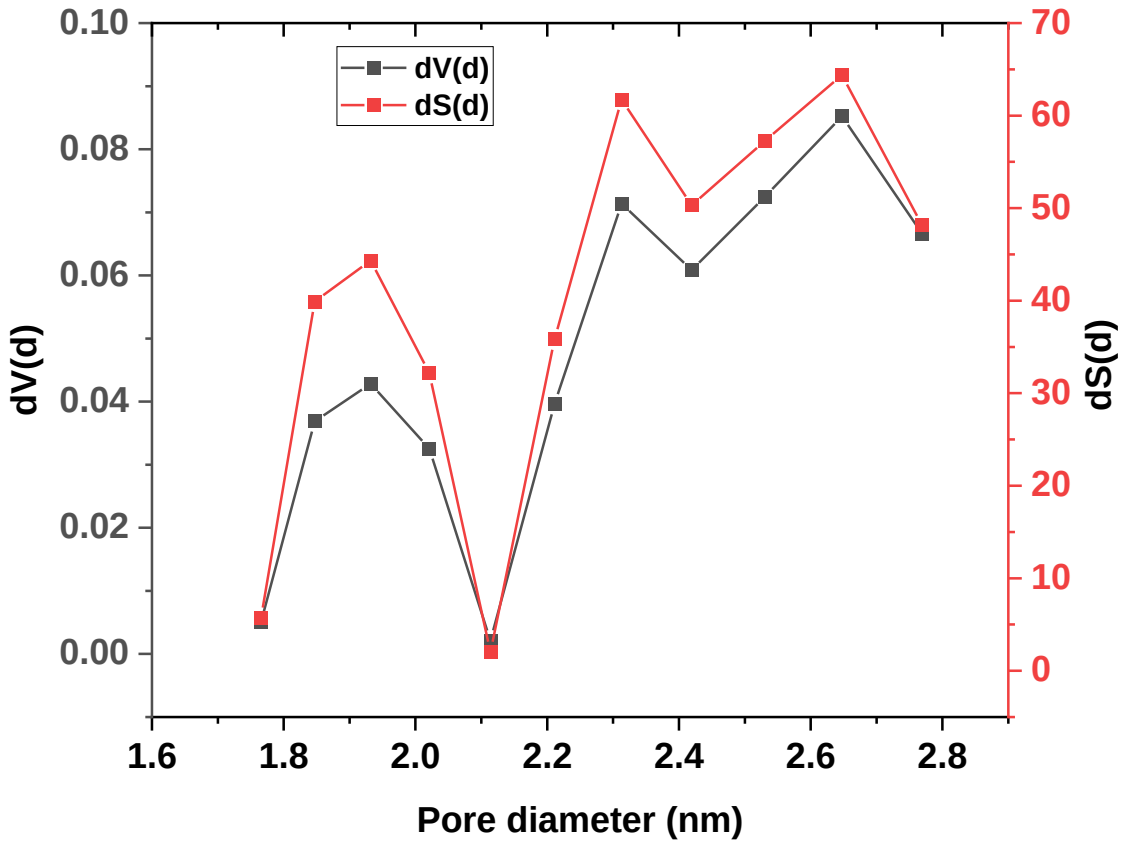

Fig. 2: Variation of differential pore volume and differential surface area with pore diameter for the adsorption of N_2 on AgNC-L

Also, the differential surface area shows peaks at similar pore widths as dV(d), which correlates with the distribution of surface area within the pores. The highest peak in dS(d) is at 2.6472 nm with a value of 6.44E+01 $m^2/g/nm$, indicating this pore size significantly contributes to the surface area. The AgNC-L used as an adsorbent has a variety of pore sizes within the mesoporous range. The cumulative data indicates an increasing trend in both pore volume and surface area with increasing pore width. The differential data shows specific pore widths where the pore volume and surface area are most significantly distributed, highlighting the dominant pore sizes in the sample. Based on the DFT observable pore diameter for the nanoparticles AgNC-L is 2. 4776 nm, which confirms that the AgNC-L is a mesoporous material (particle size = 2 to 50 nm) with properties near the microporous zone (particle size 0 to 2 nm). The corresponding surface area of the nanoparticles was evaluated using the following equation:

$$SA(m^2/g) = \sum[(dS(d_i) \times (w_{i+1} - w_i)] \quad (1)$$

where $\boldsymbol{dS(d_i)}$is the differential surface area and $\boldsymbol{w_i}$is the pore width. The surface area calculated from the above equation is 76.30 m^2/g. Also, the pore volume was evaluated using equation 2

$$PV\ (m^3/g) = \sum[(dV(d_i) \times (w_{i+1} - w_i)] \quad (2)$$

In equation 2, $dV(d_i)$ is the differential volume. Similarly, the PV was evaluated to be equal to 0.0616 m^3/g. This implies that the surface area to volume ratio is 1238.636 m^{-1}, which is significantly large and confirms that the material is a nanoparticle.

Fig. 3 presents the plot of dV(d) versus pore diameter for the adsorption of nitrogen by AgNC-L based on the micropore model. The MIP (Micropore) method is often used to interpret and analyze nitrogen adsorption data to determine the pore size distribution and surface area of materials, particularly those with micropores (pores with diameters less than 2 nm).

The plot is based on the Dubinin-Astakhov isotherm model which can be written as shown in equation 3 (Eddy *et al*., 2023)

$$dV(d)V = V_m.\frac{1}{\sqrt{2\pi\sigma^2}}\ exp\left(\frac{\left(-ln(d)-ln(d_0)\right)^2}{2\sigma^2}\right).\frac{d}{d_0} \quad (3)$$

The definition of terms in equation 3 above are as follows, dV(d) is the differential pore volume, defined as the volume of adsorbate per unit change in pore diameter), d is the pore diameter, V_m is the maximum adsorption capacity (volume of adsorbate corresponding to complete filling of the pores), d_0 is the characteristic pore diameter (related to the pore size where the adsorption is maximized) and σ is the width of the pore size distribution (standard deviation of the log-normal distribution).

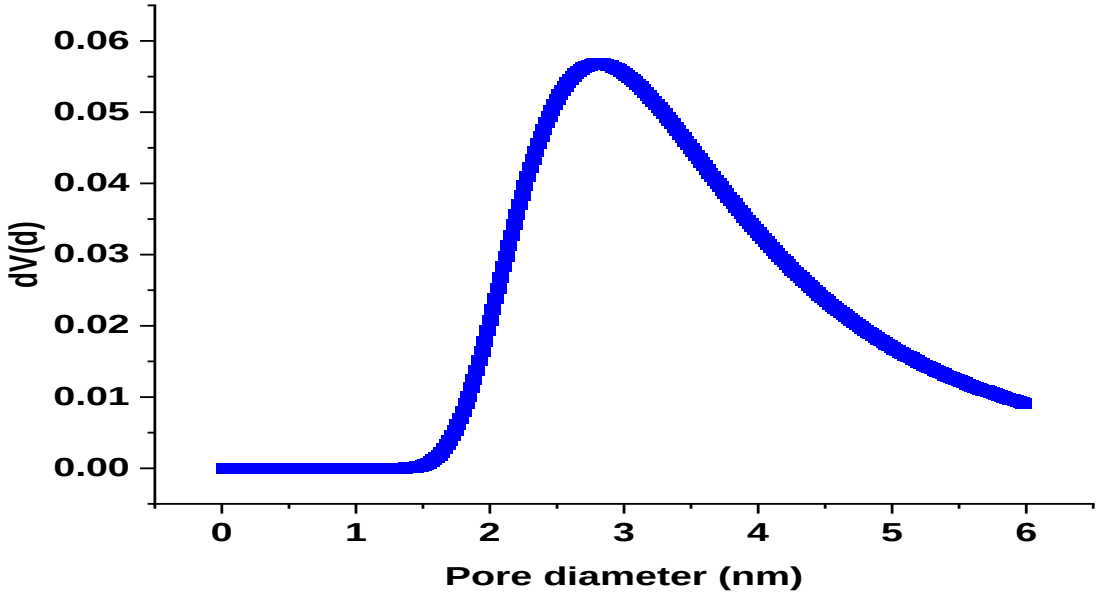

Fig. 3: Plot showing micropore analysis of AgNC-L based on nitrogen adsorption

From Fig 3, the most frequent pore diameter of the AgNC-L is 2.78 nm, which represents the pore diameter of the nanoparticles. Also, the shape of the DA curve (Fig. 3) provides information about the pore size distribution. A narrow peak suggests a relatively uniform pore size distribution, while a broader peak indicates a wider range of pore sizes. Since Fig. 3 indicates a relatively narrow peak, a fairly uniform pore size distribution around 2.78 nm is the pore diameter of the AgNC-L while the pore volume was obtained by integrating the dV(d) across the range of pore diameter, which is

$$\boldsymbol{V} = \int_{0.00433}^{6.0292} dV\,(d) \quad (4)$$

The result of the integration indicates that the pore volume is 0.13187 m^2/g. The surface area was evaluated based on the spherical model expressed as equation 4

$$S = 4\pi r^2 \quad (5)$$

Based on the above model, the surface area was evaluated as 97.1614 m^2/g. Consequently, the

surface area to volume ratio is 736.7968 m^{-1}. The equation representing the Langmuir model for nitrogen adsorption can be expressed in terms of pressure as follows,

$$\frac{P}{P_0} = \frac{W}{W_m}.\frac{1}{1+b.\frac{P}{P_0}} \quad (6)$$

In equation 6, W represents the amount of adsorbate (nitrogen) adsorbed at pressure P, is the maximum adsorption capacity (monolayer coverage), b is the Langmuir constant related to the affinity of the adsorbate for the surface and $\frac{P}{P_0}$ is the relative pressure. Equation 6 was re-arranged to a linear model given as equation 7.

$$\frac{P}{P_0}.\left(\frac{1}{W}\right) = \frac{1}{W_m}.\frac{P}{P_0} + \frac{b}{W_m} \quad (8)$$

The plotting of $\frac{P}{P_0}.\left(\frac{1}{W}\right)$ versus $\frac{P}{P_0}$ (Fig. 4) led to a linear plot with a corresponding slope and intercept equal to $\frac{1}{W_m}$ and $\frac{b}{W_m}$ respectively. The adsorption parameters calculated from the plots were R^2 = 0.9250, slope = 6.6653, $W_m = 2.50515 \times 10^{-5}$, $b = 1.2836$ and intercept = 4.5113. The Langmuir surface area (specific surface area) can be calculated by fitting data to equation 9 (Eddy *et al*, 2024c)

$$SSA = \frac{W_m\, A}{N \times \rho} \quad (9)$$

Based on the evaluated values of the above parameters, the SSA of the AgNC-L was calculated as 522.586 m^2/g which is slightly higher than values obtained from DFT and DA methods. We also apply the BET adsorption model (equation 10) for the adsorption of nitrogen gas on the surface of AgNC-L (Grg *et al*., 2024)

$$\frac{1}{W\left(\frac{P}{P_0}-1\right)} = \frac{C-1}{W_m C}.\frac{P}{P_0} + \frac{1}{W_m C} \quad (10)$$

The linear plot representing the BET model (based on equation 10) is shown in Fig. 5. The model shows a fitness degree of 0.9867 while the slope and intercept were 16.6466 and 4.1164 respectively. This implies that the surface area is 167.78 m^2/g

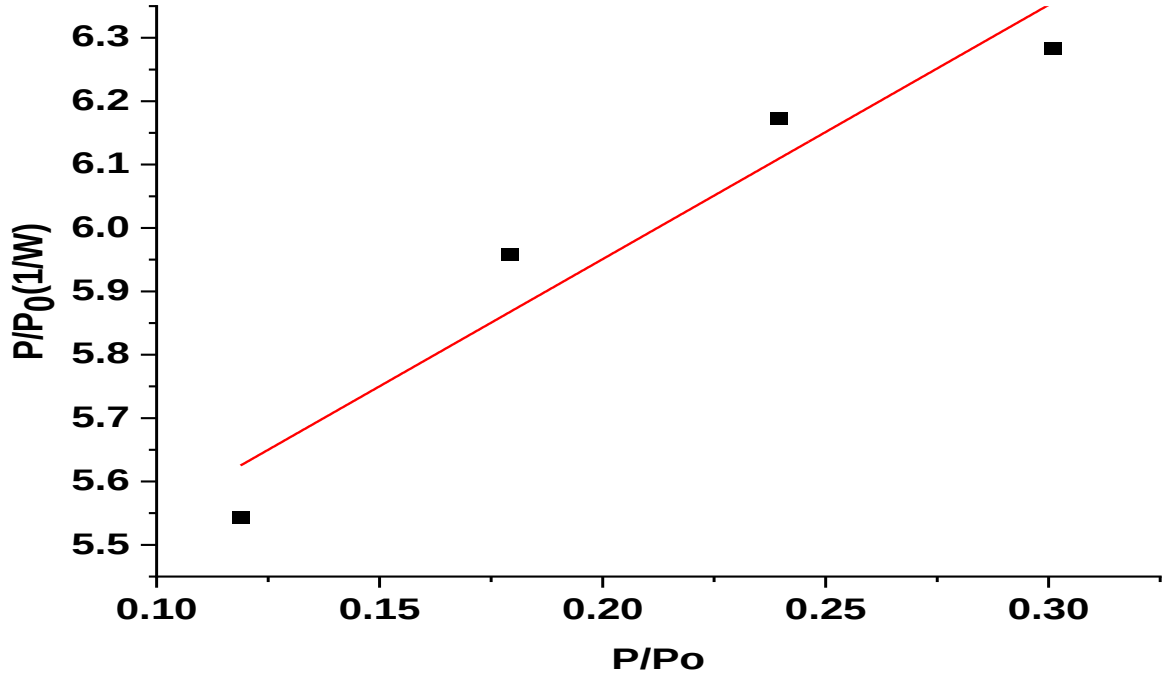

Fig. 4: The Langmuir isotherm for nitrogen adsorption by AgNC-L

4.0 Conclusion

The present study on pore parameters analysis of *Echinochloa pyramidalis* leaf-doped silver nanoparticles presents a comprehensive study on its synthesis and characterization. The research highlights the significance of AgNPs in industrial applications, particularly due to their high surface area, thermal stability, and mesoporous nature. The study successfully synthesized AgNPs doped with the plant's leaf extract and analyzed their surface and pore properties using nitrogen adsorption methods based on BET models.

The findings from this study demonstrate that the AgNPs exhibit a mesoporous structure with pore diameters ranging from 1.7656 to 2.7691 nm, with a cumulative pore volume and surface area increasing with pore width. The study also identified key pore diameters that contribute significantly to the material's surface area and pore volume, confirming that the nanoparticles possess a broad distribution of pore sizes. The Langmuir and BET models provided surface area estimates of 522.586 m^2/g and 167.78 m^2/g, respectively, further underscoring the high surface area to volume ratio of the nanoparticles.

In conclusion, the study validates the potential of *Echinochloa pyramidalis* leaf extract in synthesizing AgNPs with desirable pore properties, particularly in the mesoporous range, making them suitable for various industrial applications such as water purification and environmental remediation. The research fills a knowledge or research gap by offering a detailed analysis of the pore parameters of AgNPs synthesized using a less commonly studied plant species.

It is recommended that future studies explore the application of these AgNPs in real-world scenarios, particularly in water purification systems, to further validate their efficacy. Additionally, investigating the long-term stability and reusability of these nanoparticles in different environmental conditions would provide valuable insights into their practical applicability. Further research could also consider exploring other plant species for nanoparticle synthesis to expand the range of possible applications and enhance the understanding of plant-based green synthesis methods.

5.0 References

Ahmed, S., Ahmad, M., Swami, B. L., & Ikram, S. (2022). Green synthesis of silver nanoparticles using plants and their application as antimicrobial agents: A review. *Journal of Advanced Research*, 7, 1, pp. 17-28. https://doi.org/10.1016/j. -jare2021.09.003

Akpanudo , N. W. & Olabemiwo, O. M. (2024a).Green synthesis and characterization of copper nanoparticles (CuNPs) and composites (CuC) using the *Echinochloa pyramidalis* extract and their application in the remediation of PAHs in water. *Water Practice & Technology* 19,2, 324. doi: 10.2166/wpt.2024.011

Akpanudo, N. W. & Olabemiwo, O. M. (2024b). Synthesis and characterization of silver nanoparticles and nanocomposites using *Echinochloa pyramidalis*(Antelope grass) plant parts and the application of the nanocomposite for the removal of PAHs from bitumen seepage water. *South African Journal of Chemical Engineering*, 47, pp, 98–110.

Alshammari, S. O., Mahmoud, S. Y., and Farrag, E. S. (2023).Synthesis of green copper nanoparticles using medicinal plant Krameria sp. root extract and its applications. Molecules 28, 4629. https://doi.org/10.3390/molecules28124629.

Dauthal, P. & Mukhopadhyay, M. (2016). Noble metal nanoparticles: Plant mediated synthesis, mechanistic aspects of synthesis and applications. *Industrial and Engineering Chemistry Research*, 55 36, doi:10.1021/acs.lecr.6b00861

Dudnikova, Y. N., Zykov, I. Y., Fedorova, N. I. & Smagilov, Z. R. 2021 Adsorption method for determining the texture characteristics of Kuzbass fossil coals of the metamorphism series. *Journal of Physics: Conference Series* 1749, 012019.doi:10.1088/1742-6596/1749/1/ -012019.

Eddy, N. O., Edet, U. E., Oladele J. O., Kelle, H. I., Ogoko. E. C., Odiongenyi, A. O., Ameh, P., Ukpe, R. A., Ogbodo, R., Garg, R. & Garg, R. (2023b). Synthesis and application of novel microporous framework of nanocomposite from trona for photocatalysed degradation of methyl orange dye. *Environmental Monitoring and Assessment*, 194, 1416, doi: 10.1007/s10661-023-12014-x,

Eddy, N. O., Garg, R., Garg, R., Garg, R., Ukpe, R. A. & Abugu, H. (2024a). Adsorption and photodegradation of organic contaminants by silver nanoparticles: isotherms, kinetics, and computational analysis. *Environ Monit Assess, 196, 65, https://doi.org/10.1007/s -10661-023-12194-6.*

Eddy, N. O., Jibrin, J. I., Ukpe, R. A., Odiongenyi, A., Iqbal, A., Kasiemobi, A. M., Oladele, J. O., & Runde, M. (2024b). Experimental and theoretical investigations of photolytic and photocatalysed degradations of crystal violet dye (CVD) in water by oyster shells derived CaO nanoparticles (CaO-NP), *Journal of Hazardous Materials Advances, 13*, 100413, https://doi.org/10.1016/j.haza -dv.2024.100413.

Eddy, N. O., Ukpe, R. A., Ameh, P., Ogbodo, R., Garg, R. & Garg, R. (2023). Theoretical and experimental studies on photocatalytic removal of methylene blue (MetB) from aqueous solution using oyster shell synthesized CaO nanoparticles (CaONP-O). *Environmental Science and Pollution Research*, 30, pp. 81417-81432, https://doi.org/10.1007/s1 -1356-022-22747-w.

Garg, R., Mittal, M., Tripathi, S., & Eddy, N. O. (2024). Core to concept: synthesis, structure, and reactivity of nanoscale zero-valent iron (NZVI) for wastewater remediation. *Environmental Science and Pollution Research*.. https://doi.org/10. 1007/s11356-024-33197-x

Gupta, A., Sharma, S., & Goyal, D. (2022). Differential pore volume and surface area analysis of biosynthesized silver nanoparticles using plant extracts. *Materials TodayProceedings*, 49, 2, pp. 1216-1222. https://doi.org/10.1016/j. -matpr.2022.01.089

Jadoun, S., Arif, R., Jangid, N. K. & Meena, R. K. (2021). Green synthesis of nanoparticles using plant extracts: a review. *Environmental Chemistry Letters* 19, pp. 355-374. doi:10.1007/s10311-020-01074x

Jalab, J., Abdelwahed, W., Kitaz, A., & Al-Kayali, R. (2021). Green synthesis of silver nanoparticles using aqueous extract of *Acacia cyanophylla* and its antibacterial activity. *Heliyon*, 7, 5, e08033. doi:10.1016/j.heliyon.2021.e080 -33

Khan, Z., Hussain, J., & Ali, S. (2020). Synthesis and applications of silver nanoparticles: A review. *Environmental Chemistry Letters*, 18, 2, pp. 295-315. https://doi.org/10.1007/s10311-019-0099 5-5

Lee, Y. J., Park, J. Y., & Kang, H. K. (2019). Catalytic activity of mesoporous silver nanoparticles for environmental remediation. Catalysis Science & Technology, 9(, 12, pp. 3035-3042. https://doi.org/10.1039/C8CY02387A.

Mishra, S., Singh, H., & Prasad, S. (2021). BET & DFT analysis of surface properties of biosynthesized silver nanoparticles. *Journal of Nanomaterials*, 8456723. https://doi.org/10.1155/2021/ -8456723

Nazir, S., Zhang, J. M., Junaid, M., Saleem, S., Ali, A., Ullah, A. &Khan, S. (2024). Metal- based nanoparticles: basics, types, fabrications and their electronic applications. *Zeitschrift für Physikalische Chemie* 238, doi:10.1515/zpch-2023-0375

Nkosi, N. C., Basson, A. K., Ntombela, Z. G., Dlamini, N. G., & Pullabhotla, R. V. S. R. (2024). Green synthesis, characterization and application of silver nanoparticles using bioflocculant: A review. *Bioengineering*, 11(5),492. https://doi.org/10.3390/bioengineering11050492.

Ogoko, E. C., Kelle, H. I., Akintola, O. & Eddy, N. O. (2023).Experimental and theoretical investigation of *Crassostrea* gigas (gigas) shells based CaO nanoparticles as a photocatalyst for the degradation of bromocresol green dye (BCGD) in an aqueous solution. *Biomass Conversion and Biorefinery*.https://doi.org/10.1007/s13399-023-03742-8.

Rather, M. A., Deon, P. J., Gupta, K., Daimary, N., Deka, D., Qureshi, A., Dutta, T. K., Joardar, S. N., & Mandal, M. (2022). Ecofriendly phytofabrication of silver nanoparticles using aqueous extract of Cuphea Carthagenensis and their antioxidant potential and antibacterial activity against clinically important human pathogens. *Chemosphere* 300, 134497. https://doi.org/10.1016/j.chemosphere.2022.134497

Singh, R., Singh, D., & Singh, H. (2021). Green synthesis of silver nanoparticles using plant extracts and their applications: A review. Environmental Nanotechnology, Monitoring & Management, 16, 100462. https://doi.org/10.1016/j.enmm.2021.100462.

Zhang, X., Liu, Z., & Chen, Y. (2020). Adsorption capacity of biosynthesized silver nanoparticles for water treatment applications. Journal of Environmental Management, 261, 110235. https://doi.org/10.1016/j.jenvman.2020.110235.

Compliance with Ethical Standards Declaration

Ethical Approval

Not Applicable

Competing interests

The authors declare that they have no known competing financial interests

Funding

This work was supported by the Federal Government of Nigeria need assessment fund through the Akwa Ibom State University.

Availability of data and materials

Data would be made available on request.

Authors Contribution

Both authors contributed to the work. The design of the work was done by both authors. Akpanudo carried out the experimental aspect of the work while Olabemiwo supervised all aspects of the work including manuscript development